DATA-INSPIRED SIMULATIONS OF THE INITIATION AND EARLY EVOLUTION OF CMEs

Francesco P. Zuccarello

Centre for mathematical Plasma Astrophysics, KU Leuven

francesco.zuccarello@wis.kuleuven.be

Outline

- Introduction
  - CME definitions
  - Shear & flux cancellation
- CME initiation in AR 9415
  - AR morphology & evolution
    - WL, Hα, Trace and MDI evolution
  - Simulation
    - Initial configuration
    - Twisting phase
    - Eruption Phase
    - Three part structure
    - Energy
    - Topology
- CME deflection
  - Observations
    - STEREO/SECCHI
    - SOHO/MDI
    - Magnetic helicity
  - Simulation
    - Initial configuration
    - Dynamical evolution
    - Three-part structure
    - Radial & Latitudinal evolution
    - The role of the global field
- Conclusions

Introduction

- CMEs are huge expulsions of magnetized plasma into the interplanetary medium (Mass: 10^{13} -10^{16} g).
- CMEs often show a three-part structure.
- When CMEs are directed towards the Earth they are called halo CMEs.

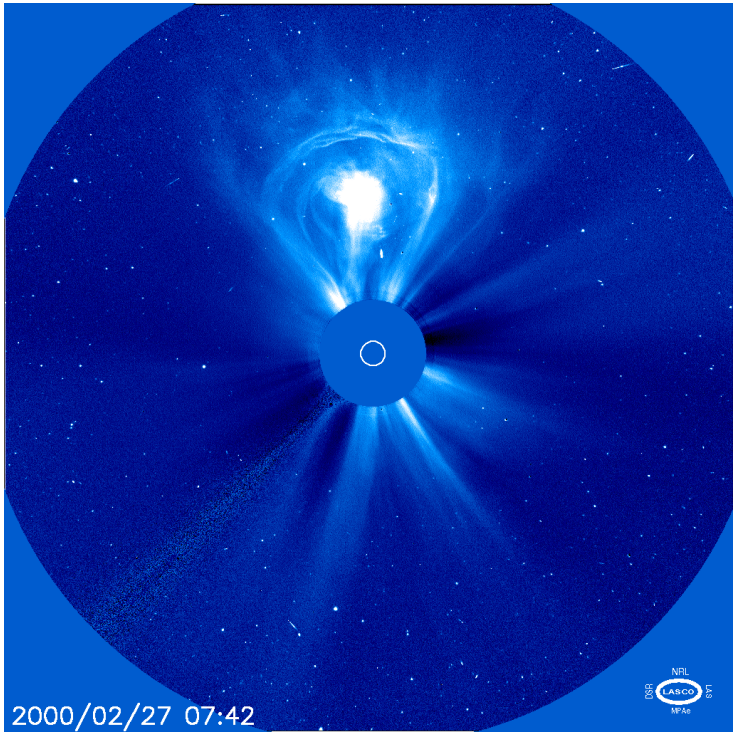

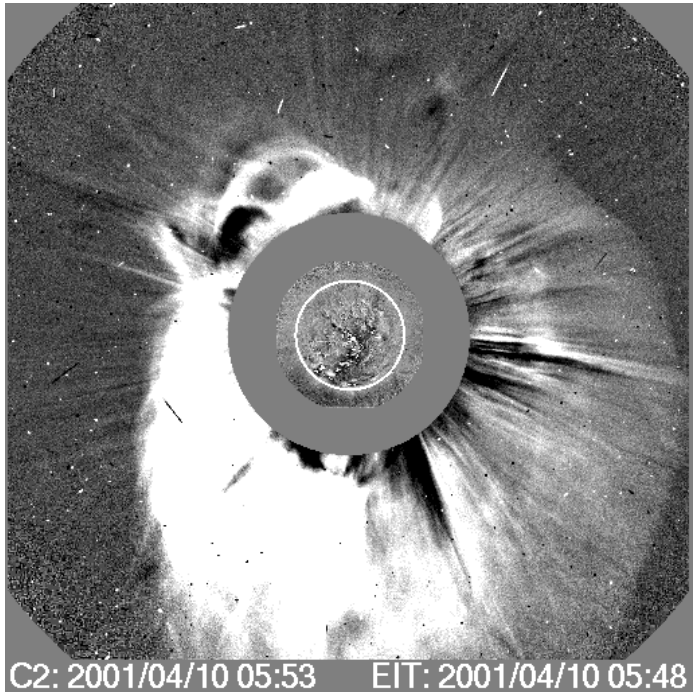

Introduction

➢ Observations show that quite often, CMEs and flares occur in the presence of highly sheared magnetic fields (Asai et al. 2009).

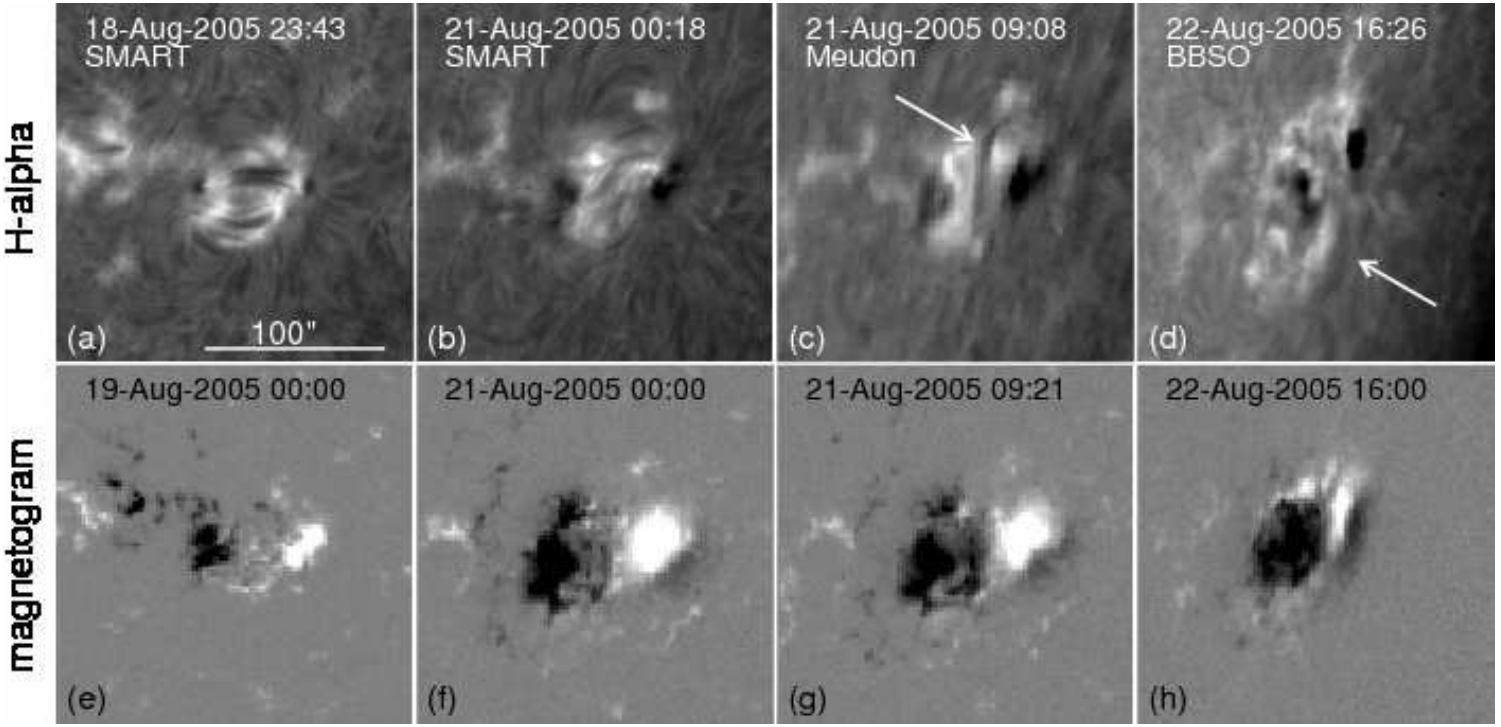

Introduction

➢ Observations show that quite often, CMEs and flares occur in the presence of highly sheared magnetic fields (Li et al. 2007).

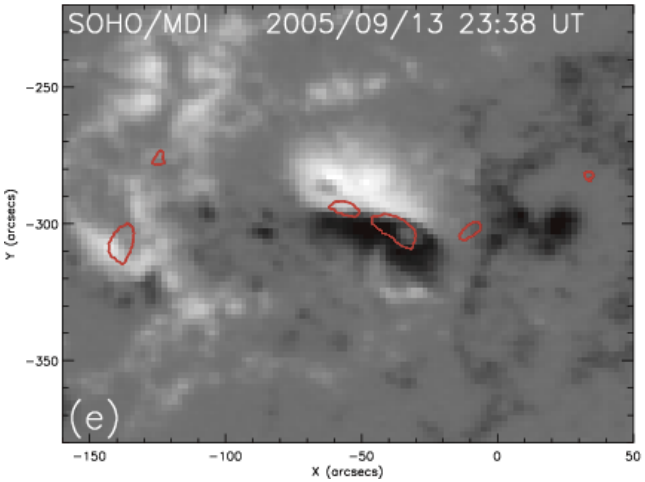

2005/09/13 23:13 UT

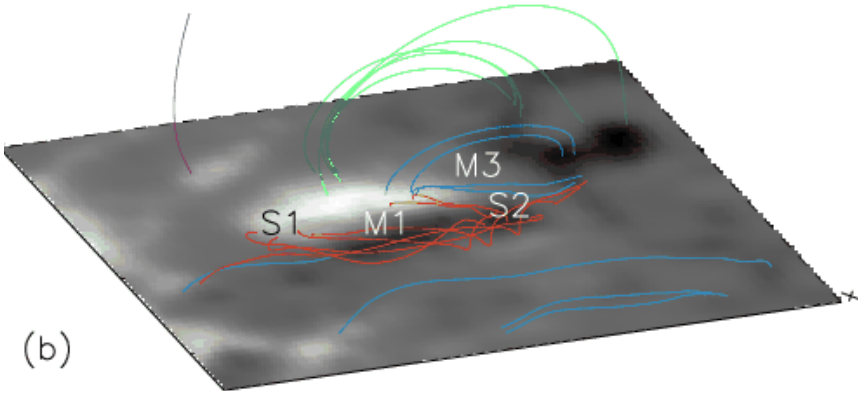

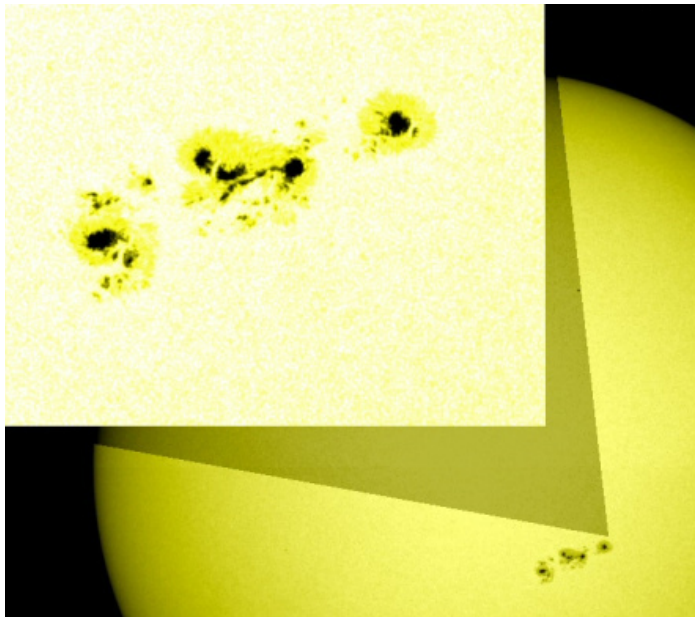

Flux cancellation (Observations)

➢ Photospheric convergence motions toward the PIL, resulting in flux cancellation events, are also often observed to precede flares and CMEs (Green et al. 2011) .

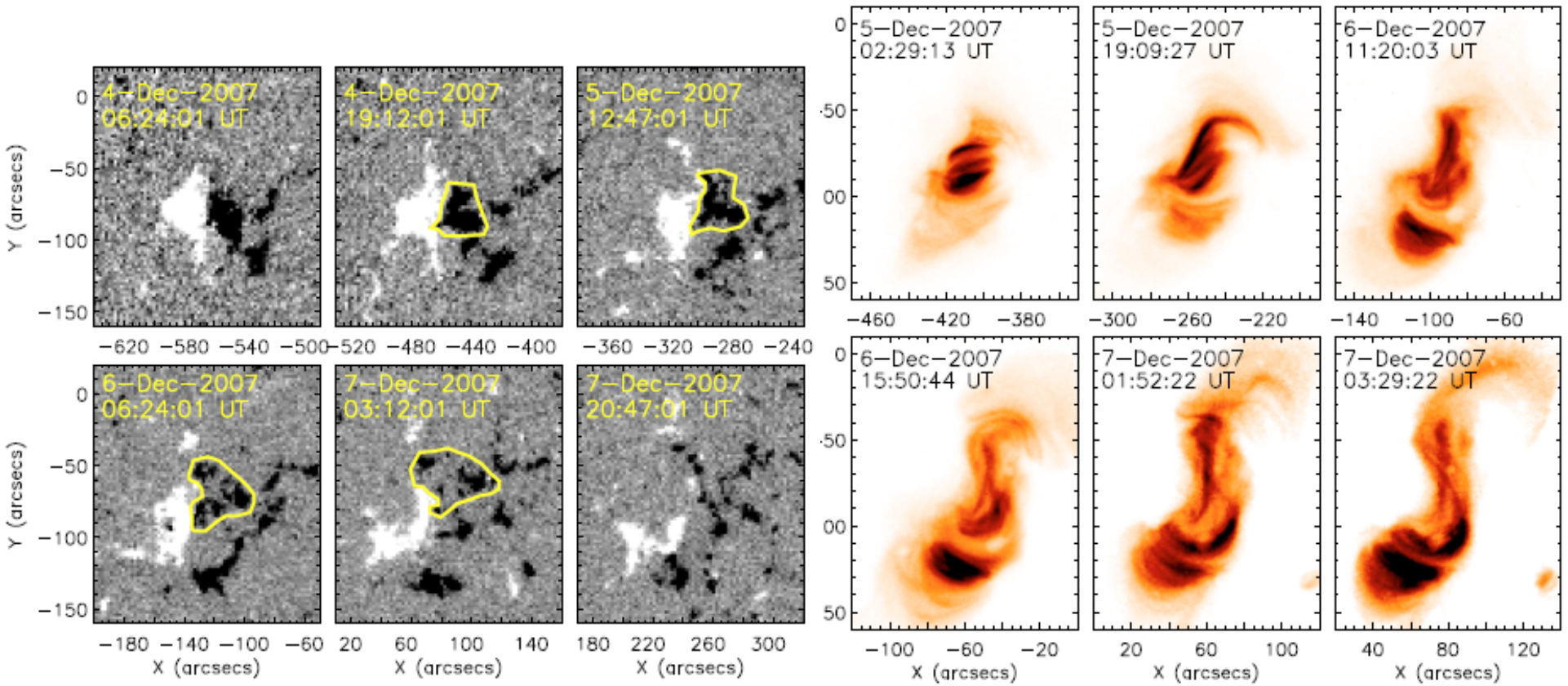

Flux cancellation (Observations)

➢ Sterling et al. (2010) concluded that the tether-cutting reconnection driven by convergence motions toward the PIL may have led to a filament ejection on 2007 May 20.

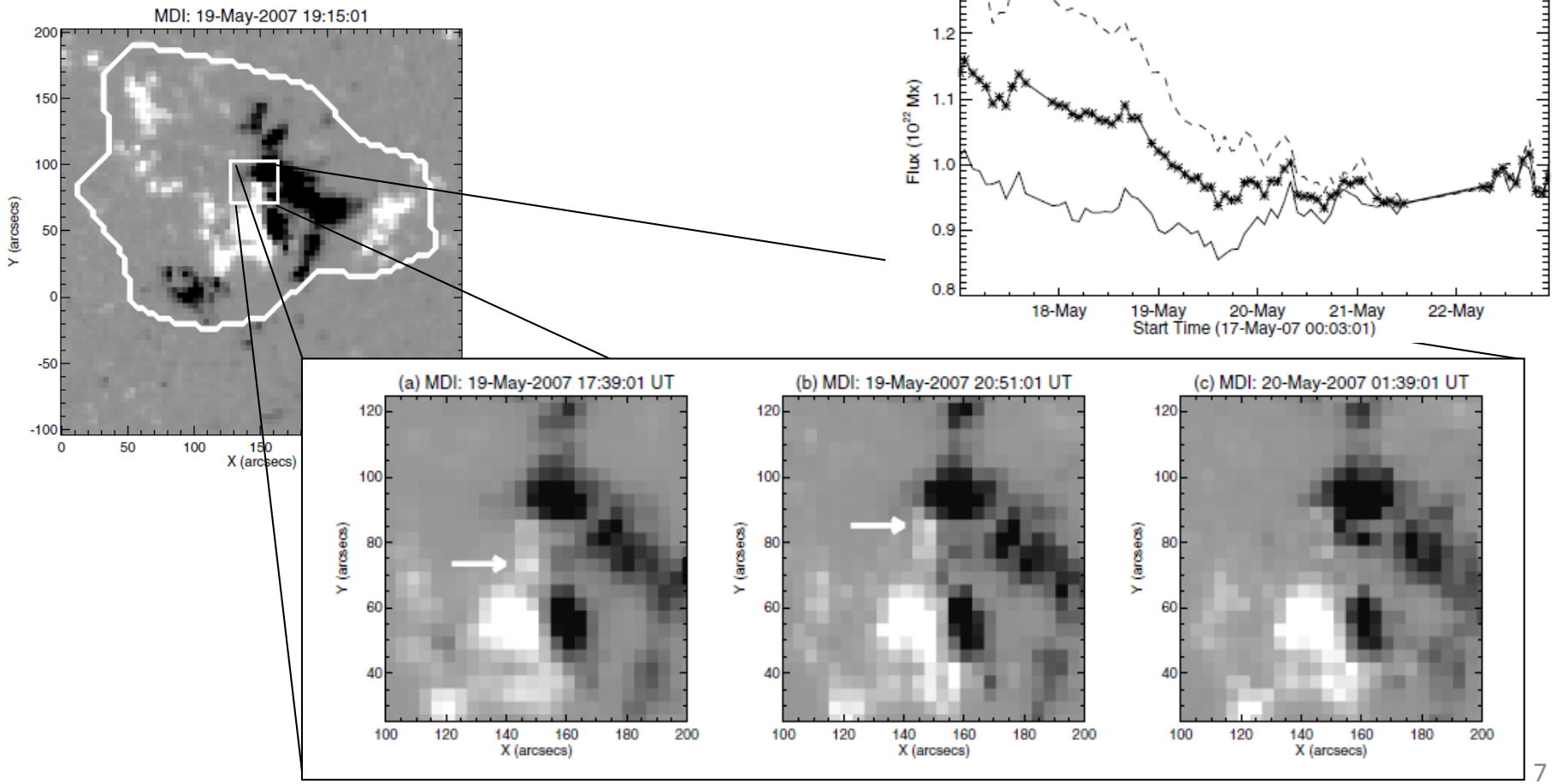

Flux cancellation (Modeling)

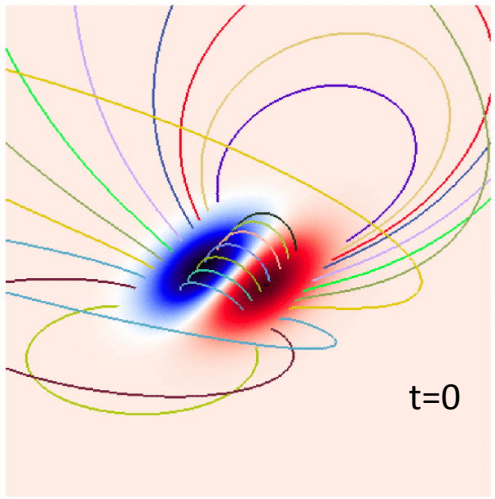

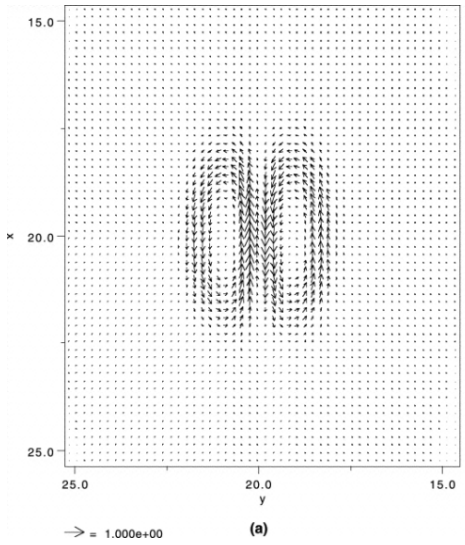

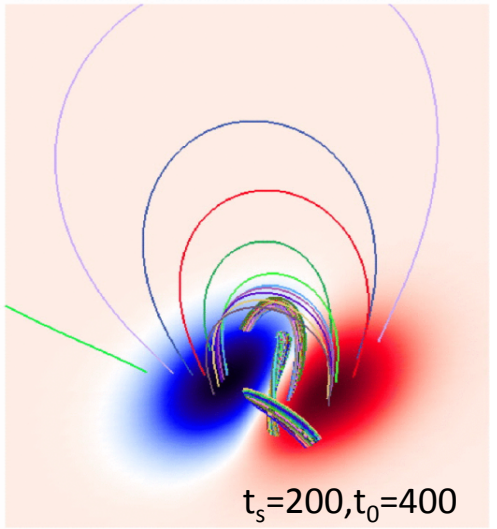

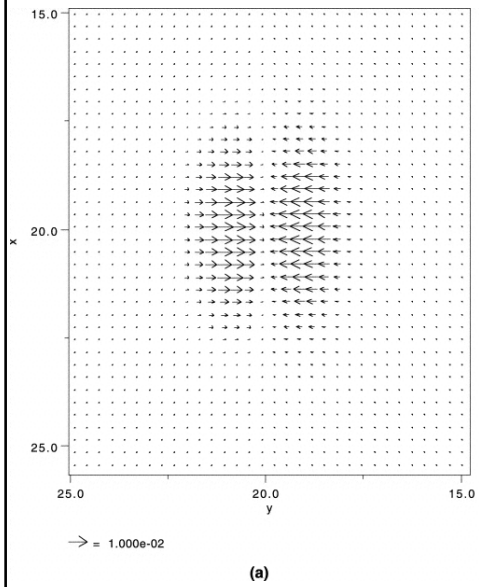

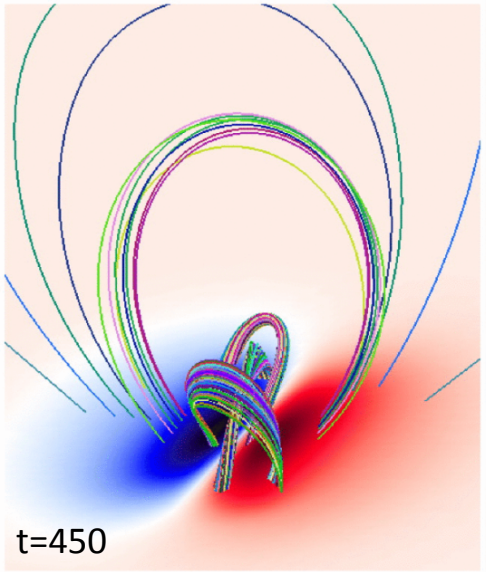

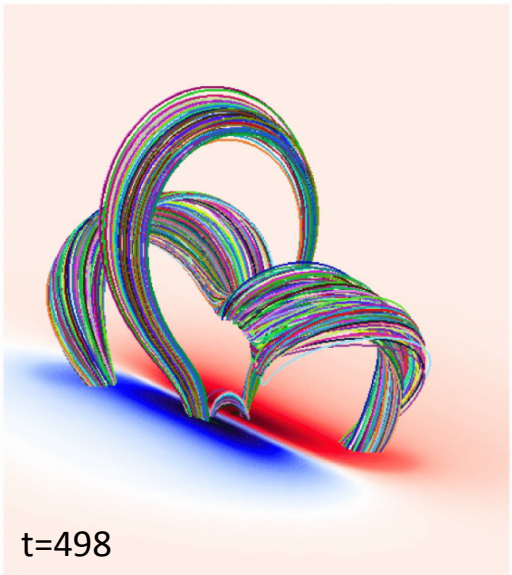

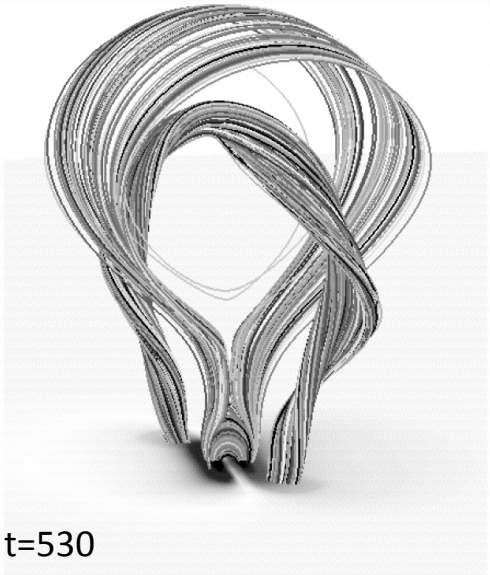

Amari et al. 2003, 2010, 2011.

Outline

- Introduction
  - CME definitions
  - Flux cancellation
- CME initiation in AR 9415
  - AR morphology & evolution
    - WL, Hα, Trace and MDI evolution
  - Simulation
    - Initial configuration
    - Twisting phase
    - Eruption Phase
    - Three part structure
    - Energy & Velocity
    - Topology
- CME deflection
  - Observations
    - STEREO/SECCHI
    - SOHO/MDI
    - Magnetic helicity
  - Simulation
    - Initial configuration
    - Dynamical evolution
    - Three-part structure
    - Radial & Latitudinal evolution
    - The role of the global field
- Conclusions

AR 9415 morphology & evolution

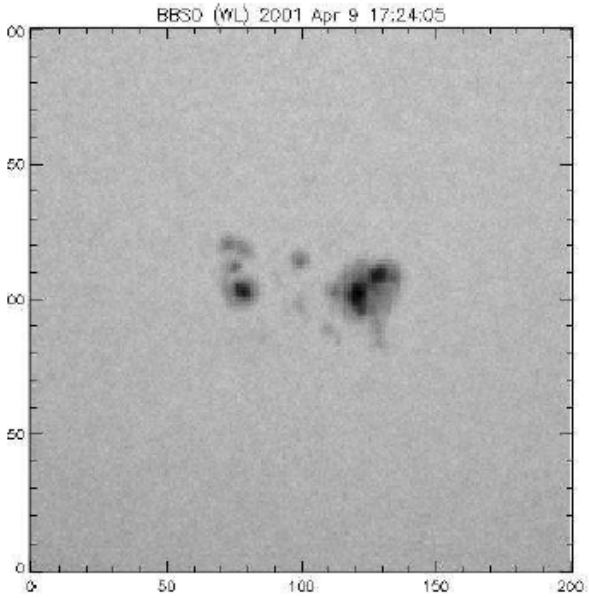

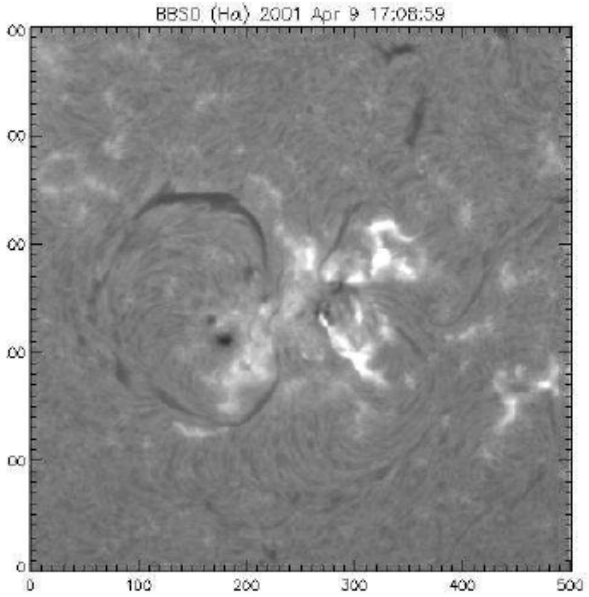

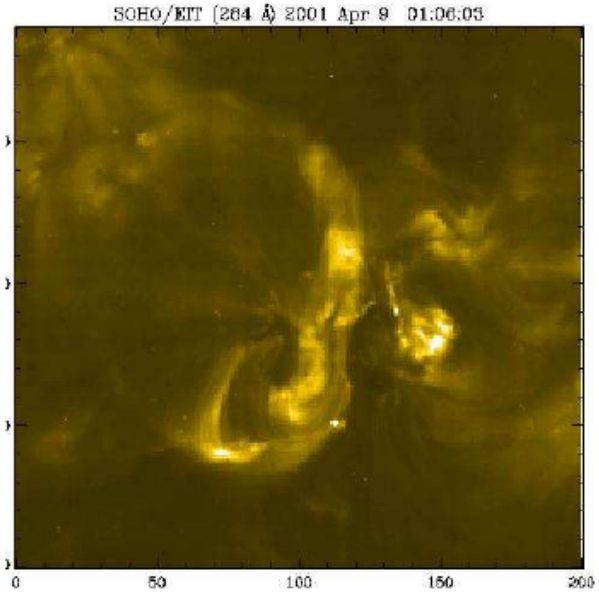

- AR NOAA 9415 appeared on the east limb of the Sun at a latitude of about 22° S.
- Many filaments are present in the AR.
- The preceding sunspots are characterized by magnetic field of opposite polarities, forming a δ-spot.
- The following sunspot has a positive flux distribution and is surrounded by a larger ring of the same magnetic polarity.
- Asymmetric convergence shearing motions are observed.

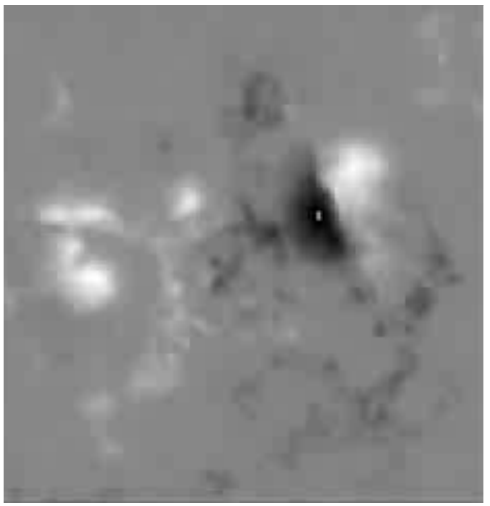

Initial condition

- The full set of non-zero plasma-β ideal-MHD equations, including the gravitational term, is solved in a Cartesian domain covering the solar corona from 1.1 R_0 to 1.9 R_0.
- As an initial condition for the magnetic field a potential field extrapolations of AR 9415 is performed.
- The extrapolated magnetic field is superimposed to an isothermal, $T_0 = 1.5 \times 10^6$ K, hydrostatic equilibrium, and the plasma density at the base of the corona is fixed to $\rho(z=0)=1 \times 10^{-16}$ g cm^{-3}.

Initial condition (II)

- Similar to the MDI magnetogram, the field distribution is characterized by three flux concentrations.
- As a consequence of the limited number of modes that we use, the small-scale structures are not reproduced in the extrapolated magnetogram.
- The field lines shown extend up to a height of about 1.25 R_0.
- The plasma-β < 1 up to 1.25R_0, however, due to the scaling of the magnetic field the plasma-β > 1 higher up in the numerical domain.
- Minor currents are generated as a consequence of the interaction between the plasma and the magnetic field.

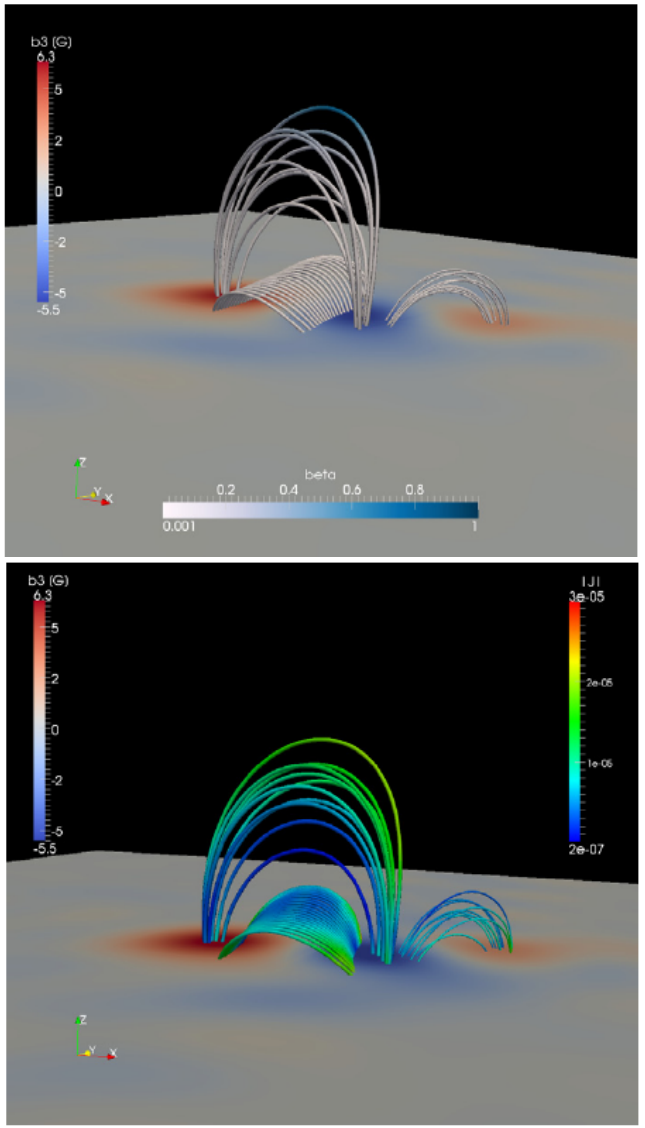

Twisting phase

- A non-linear-force-free (NLFF) equilibrium is obtained by applying vortex motions along the isocontours B_z.
- Flows along the magnetic field are generated as a response of the plasma to the driving mechanism. Moreover, as consequence of the twisting motions a slight inflation of the arcade is observed. However, this expansion is far slower when compared to the eruption phase.
- The obtained NLFF equilibrium has the same chirality as the observed AR.

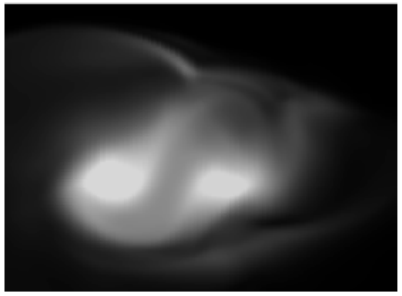

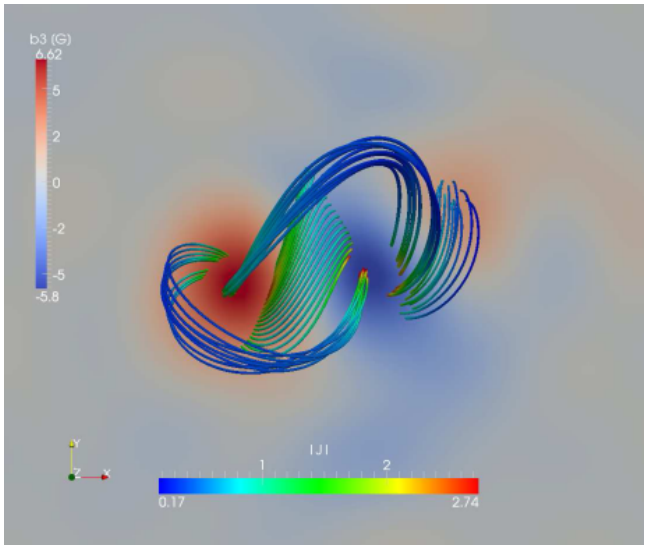

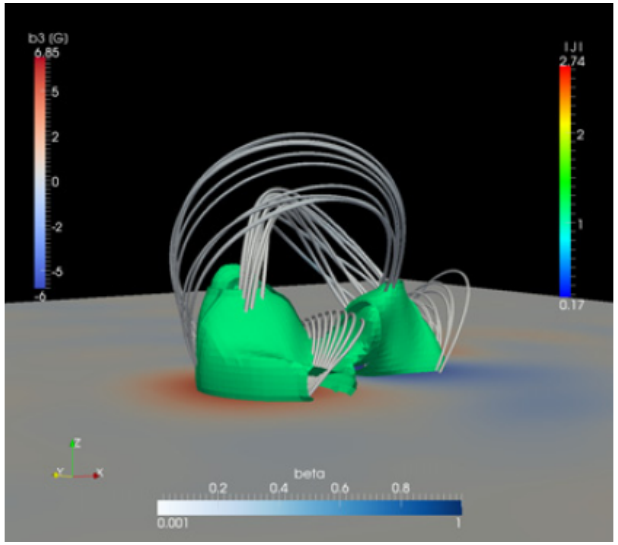

Eruption phase (I)

- Asymmetric convergence motions toward the polarity inversion line, resembling the observed ones, are applied to the positive following polarity.
- Flux is transported towards the PIL and magnetic reconnection sets in between the highly sheared field lines forming a current-carrying flux rope with both foot points anchored in the low corona.

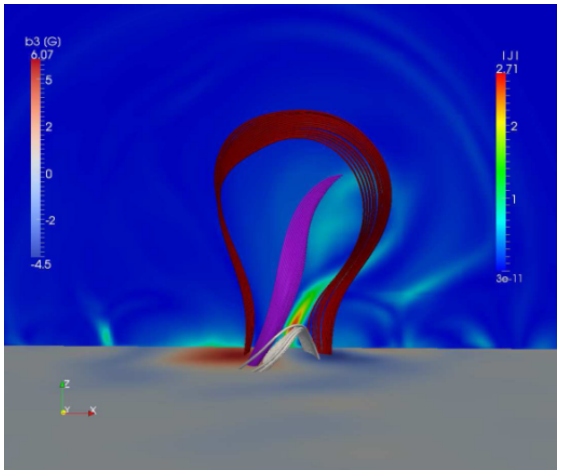

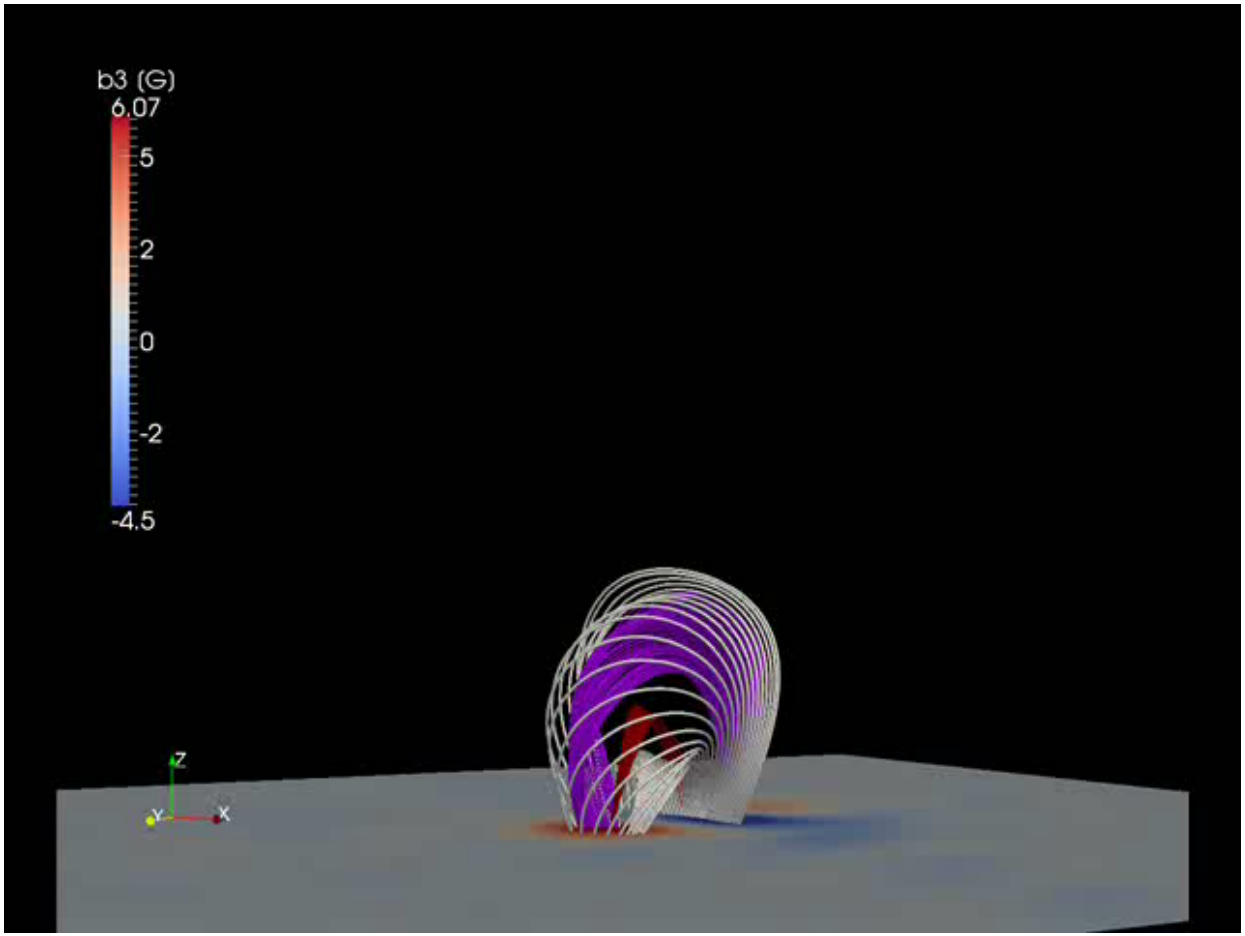

Eruption phase (II)

- As a consequence of the tether-cutting reconnection overlying flux is transferred into flux rope flux, eventually driving the eruption.
- Current J-shaped features continue to approach and eventually will merge after about 340 t_A, when a significant amount of the overlying field has been transferred to the flux rope.
- The flux rope presents a quite fragmented structure. Supersonic flows around the flux rope generate a shock that compresses the magnetic field generating a current layer where a change in the magnetic field topology can occur.
- After t = 450 t_A, the convergence motions are linearly switched off and the system is let to evolve.
- Due to the higher magnetic pressure, the flux rope continues to move upward, eventually interacting with the overlying magnetic field.

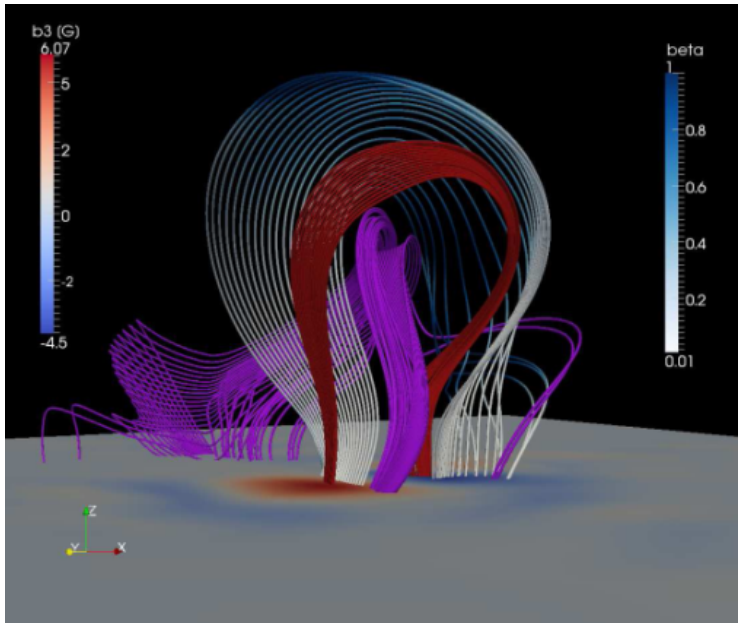

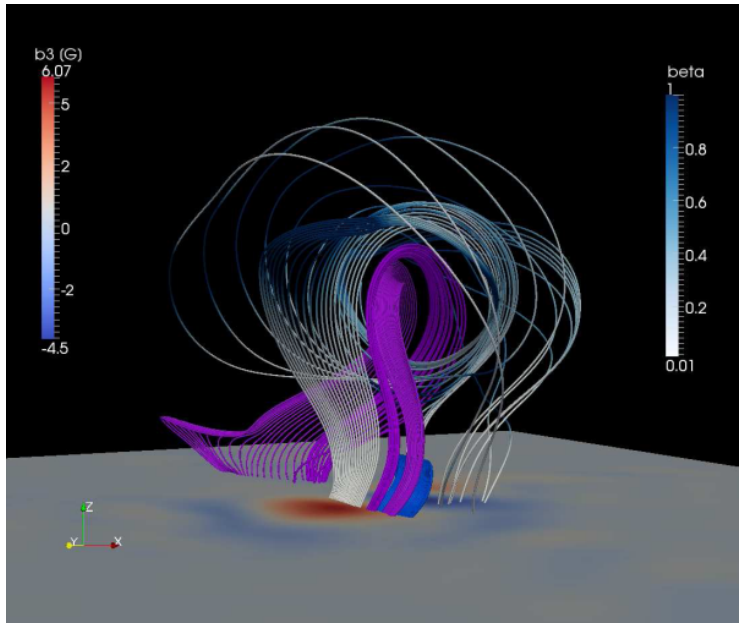

Three-part structure

- After 700 t_A, the null point separates the flux rope field from the post-flare loops that are approaching a more potential state.
- Within the flux rope, an increase in the current density is observed.
- In front of the flux rope, a mushroom-shaped current layer is formed. This is spatially correlated with the shock and with the transition between a medium where the β<1 to a medium where β>1.
- During the upward propagation of the flux rope a compressed leading edge associated with the shock front is formed.
- Within the flux rope an increase plasma density is observed resulting in a three-part structure CME.

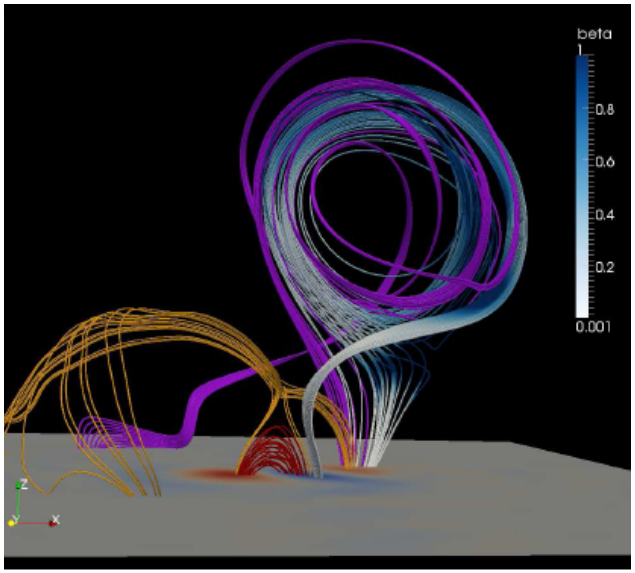

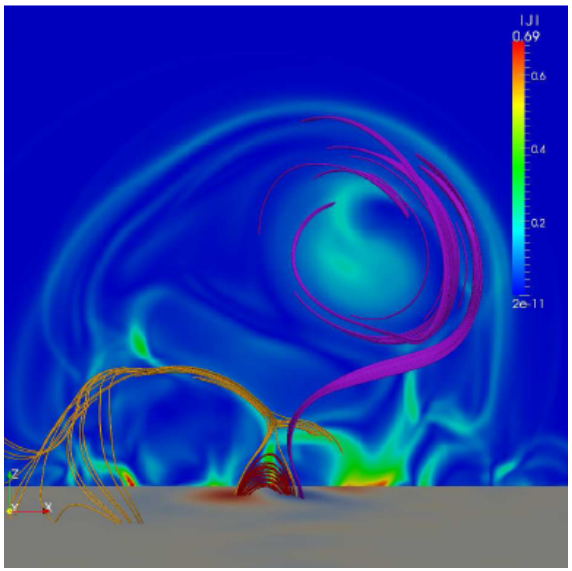

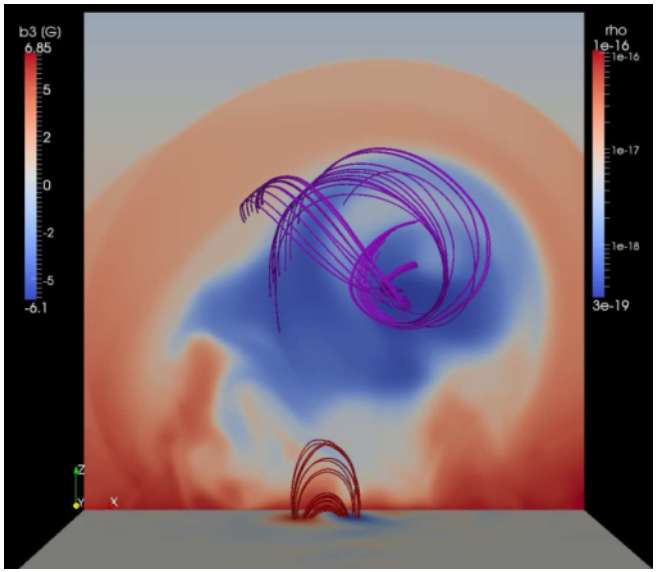

Topology

- The CME propagates in a medium where the plasma-β is higher than one; however, during its propagation, the CME perturbs the surrounding medium and due to the higher, with respect to the background, magnetic field carried within the flux rope and to the density depletion, within the CME volume the plasma-β ~ 0.1.

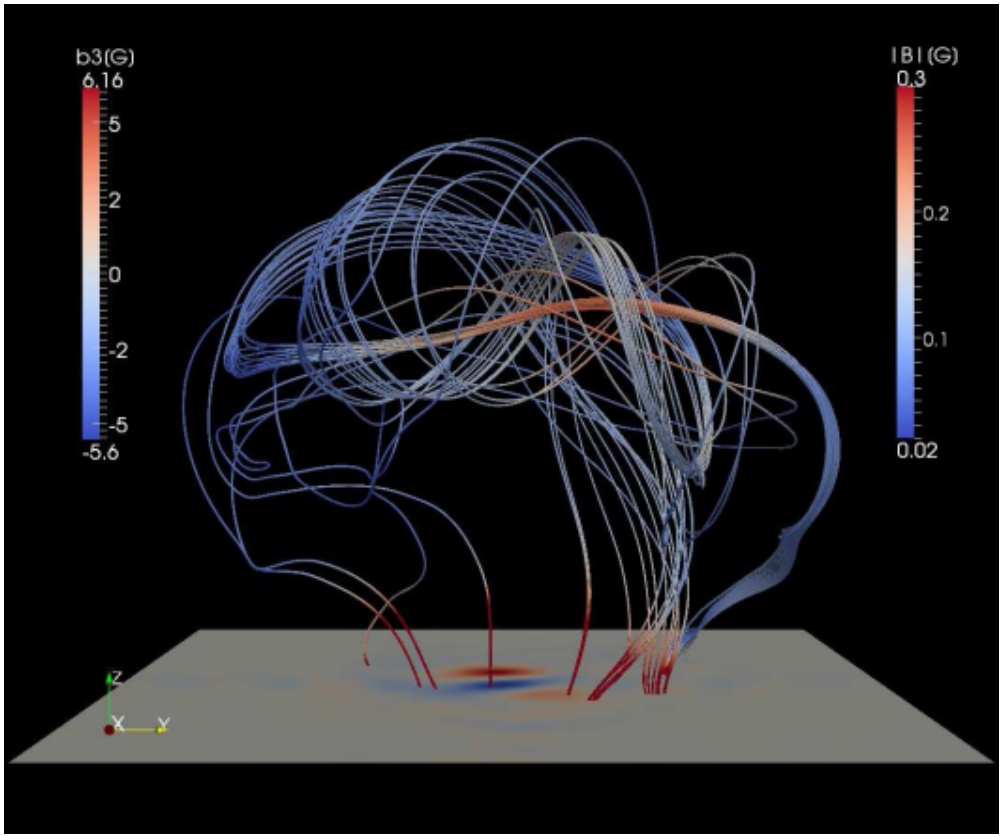

Topology

- The CME propagates in a medium where the plasma-β is higher than one; however, during its propagation, the CME perturbs the surrounding medium and due to the higher, with respect to the background, magnetic field carried within the flux rope and to the density depletion, within the CME volume the plasma-β ~ 0.1.
- Field lines starting from the δ-spot show different connectivity. Light grey field lines are connected with the southern part of the negative polarity, while the light blue ones are connected with a negative polarity at the north of the positive magnetic field spot.
- This magnetic configuration may explain both the deflection and the perturbation of the second filament.

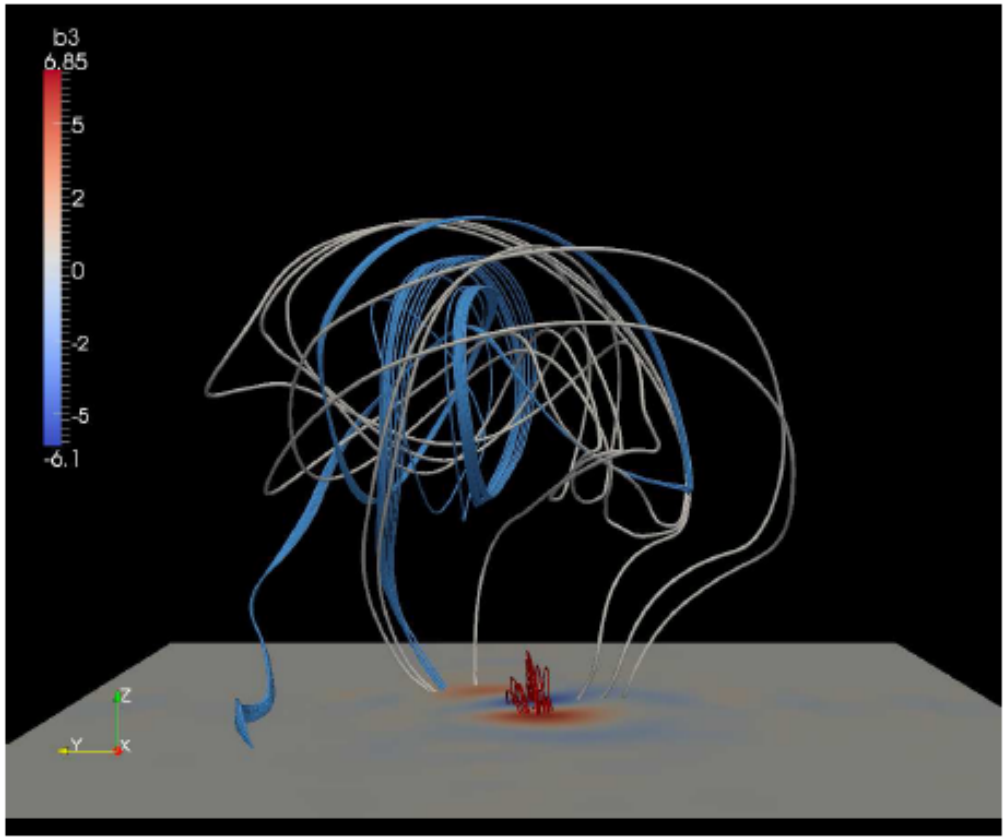

Energy evolution

- Twisting Phase: the magnetic energy (solid line) increases almost linearly up to about t = 230 t_A. Also the kinetic and internal energies increase due to the plasma motions.
- Trnsition phase, where we continuously switch from twisting to convergence motions, the magnetic energy starts to decrease.
- Convergence Phase: 170 t_A after the convergence motions began this decrease becomes even steeper and magnetic energy is converted into internal and kinetic energy.
- Finally, when the shock reaches the boundaries, the internal and the kinetic energies start to decrease.
- Significant increase in the internal energy during the flare reconnection. This increase is even more pronounced than the one in the kinetic energy, eventually supporting the relevance of heating processes during flares (Aulanier et al. 2012).

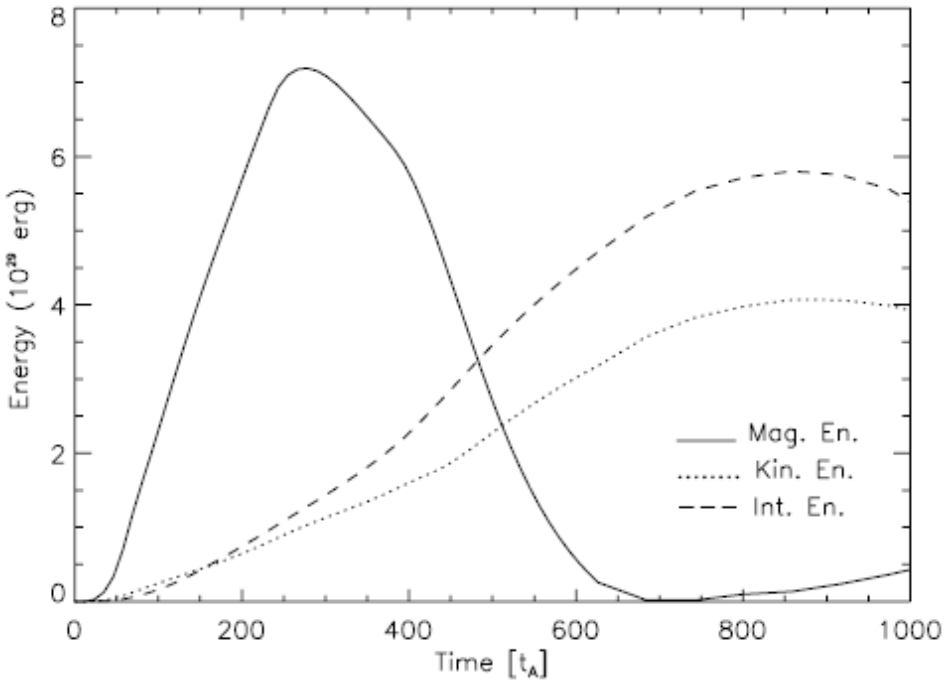

Outline

- Introduction
  - CME definitions
  - Flux cancellation
- CME initiation in AR 9415
  - AR morphology & evolution
    - WL, Hα, Trace and MDI evolution
  - Simulation
    - Initial configuration
    - Twisting phase
    - Eruption Phase
    - Three part structure
    - Energy & Velocity
    - Topology
- CME deflection
  - Observations
    - STEREO/SECCHI
    - SOHO/MDI
    - Magnetic helicity
  - Simulation
    - Initial configuration
    - Dynamical evolution
    - Three-part structure
    - Radial & Latitudinal evolution
    - The role of the global field
- Conclusions

EUVI evolution

- On 2009 September 21 at ~11:00 UT the prominence starts to rise and at ~15:00 UT it undergoes a rapid expansion.

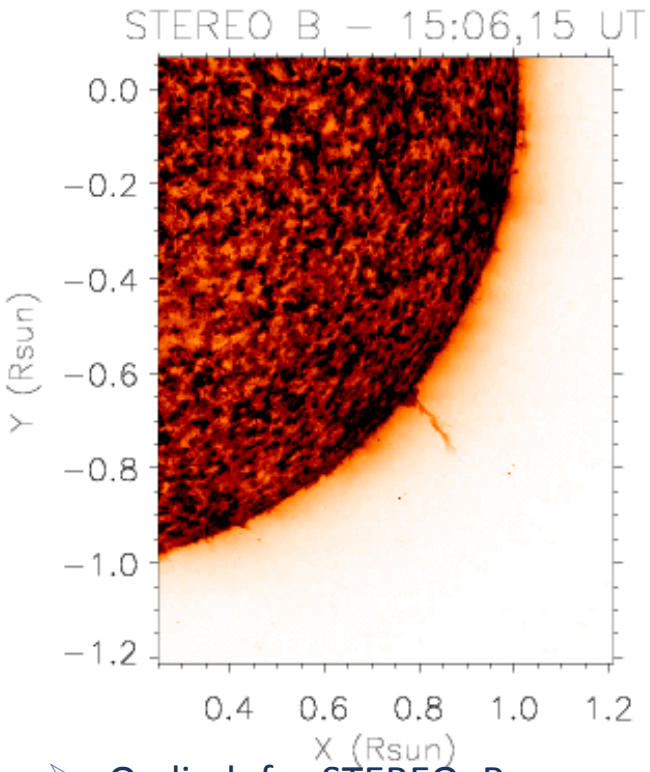

- On limb for STEREO–B

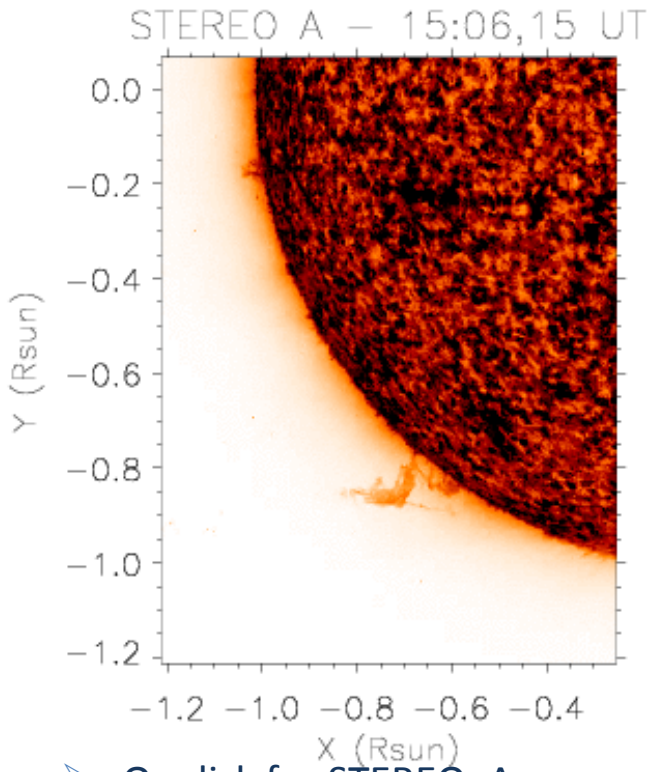

- On disk for STEREO–A
- Failed eruption

COR1 evolution

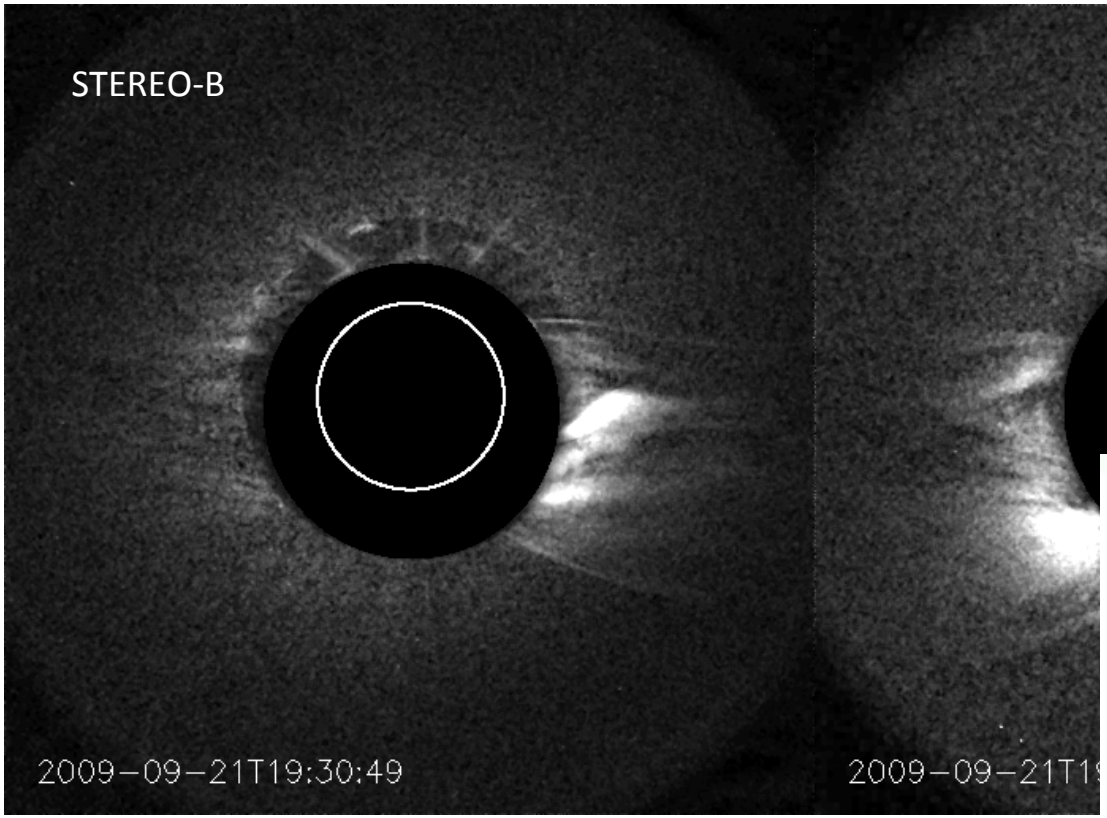

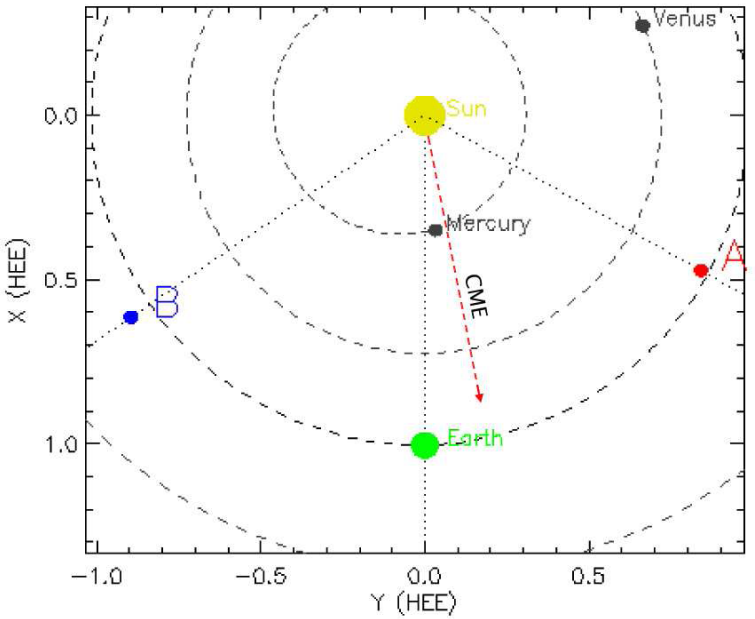

- For EUVI images we used triangulation techniques.
- For COR1 images we used the polarized ratio method together with the forward modeling in order to resolve the forward/backward ambiguity.
- The CME is in front of the POS as observed by COR1-B.

What about MDI ?

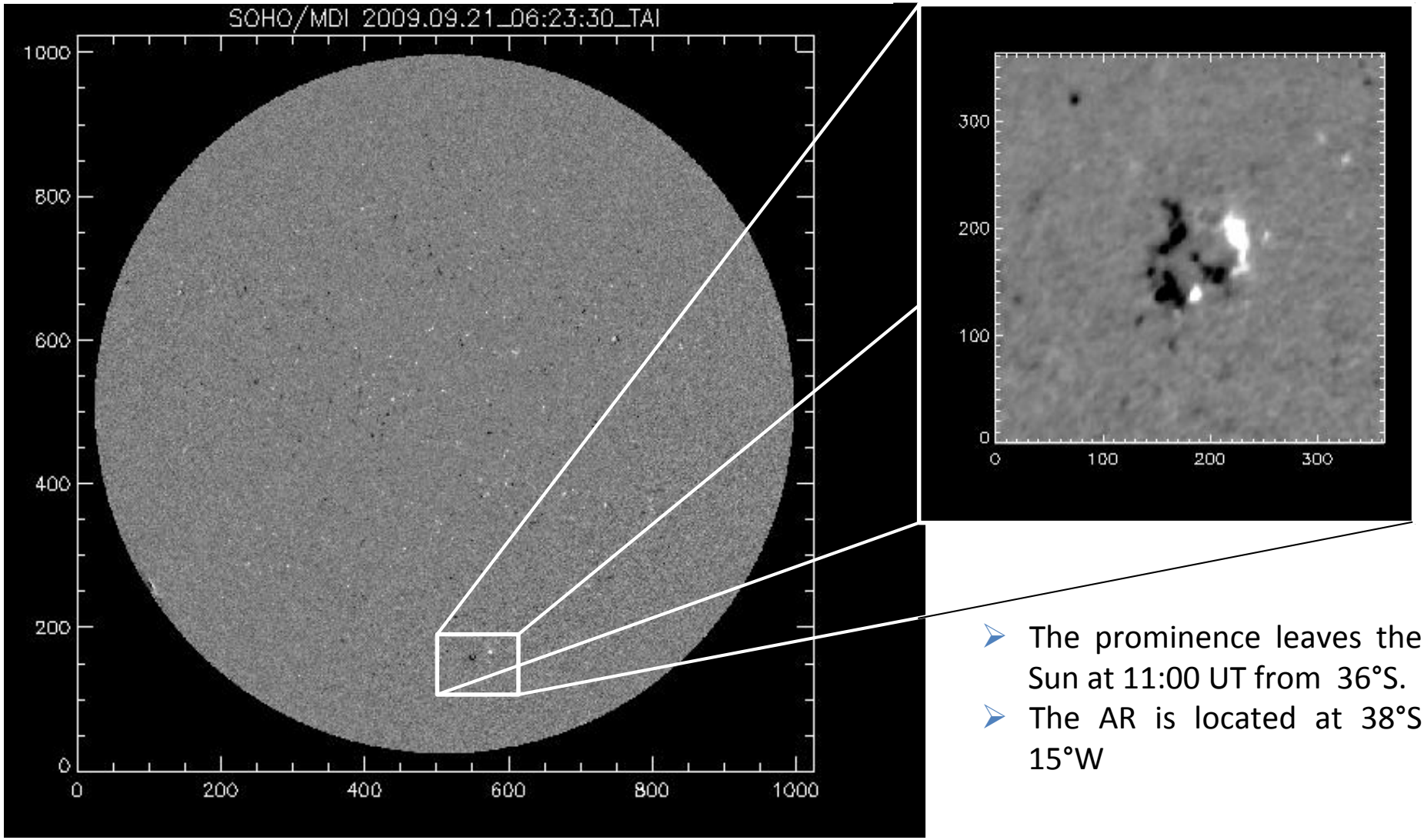

- The prominence leaves the Sun at 11:00 UT from 36°S.
- The AR is located at 38°S 15°W

What about MDI ?

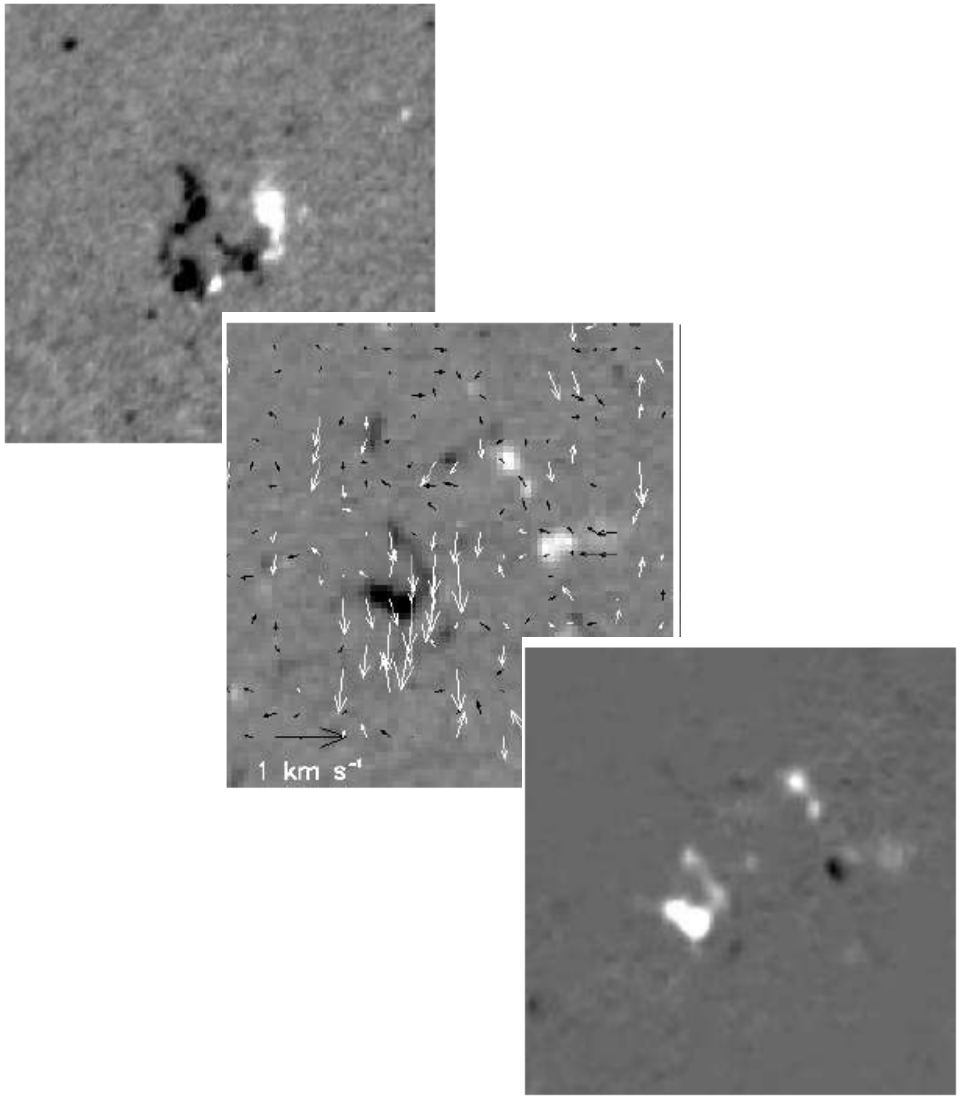

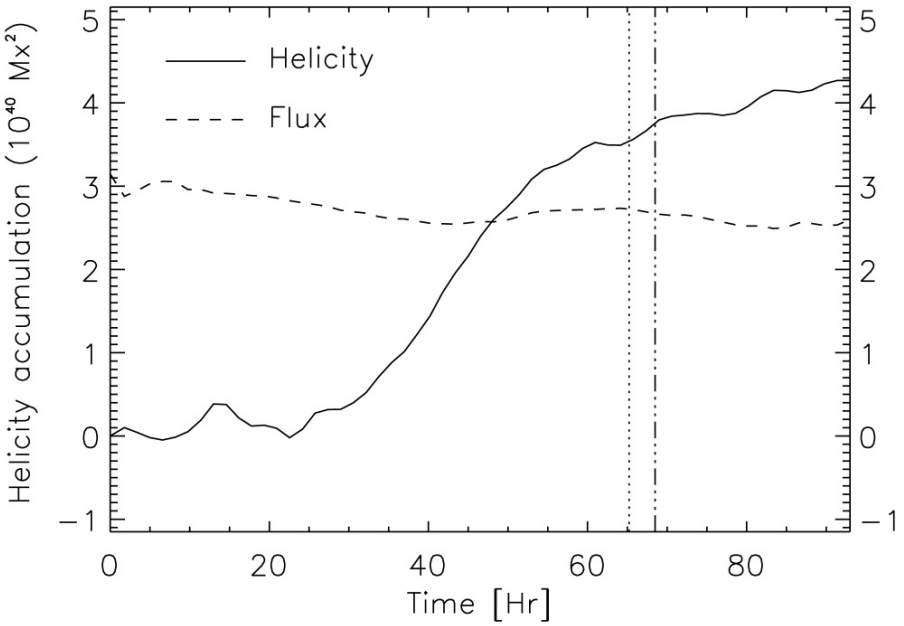

1. Consider MDI magnetograms.
2. Derive photospheric velocity maps using DAVE.
3. Derive helicity density maps.
4. Calculate helicity accumulation and magnetic flux evolution.

Steady state

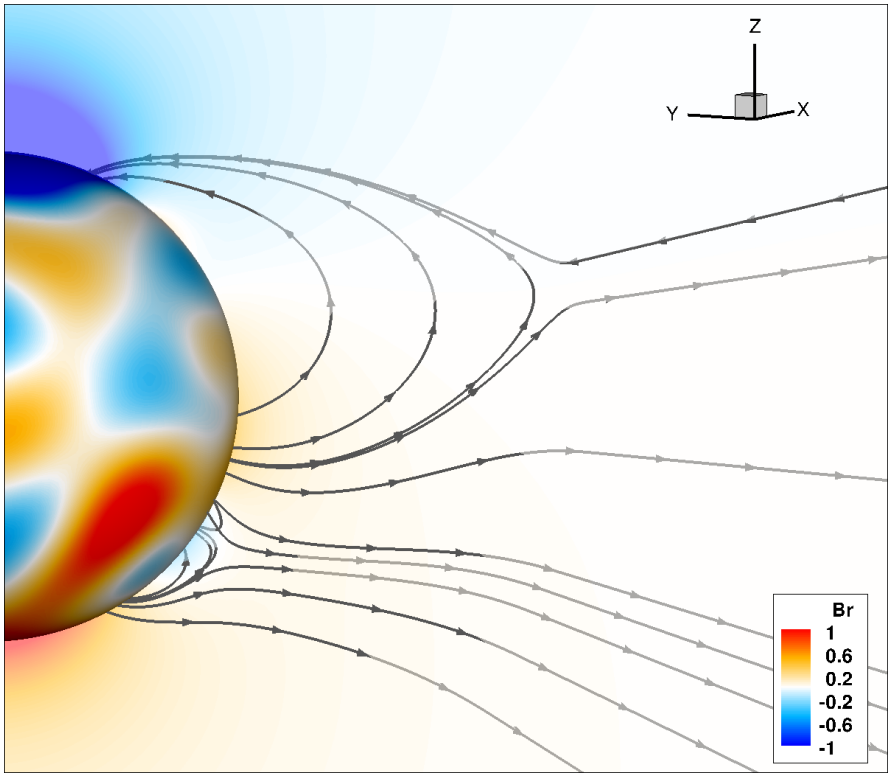

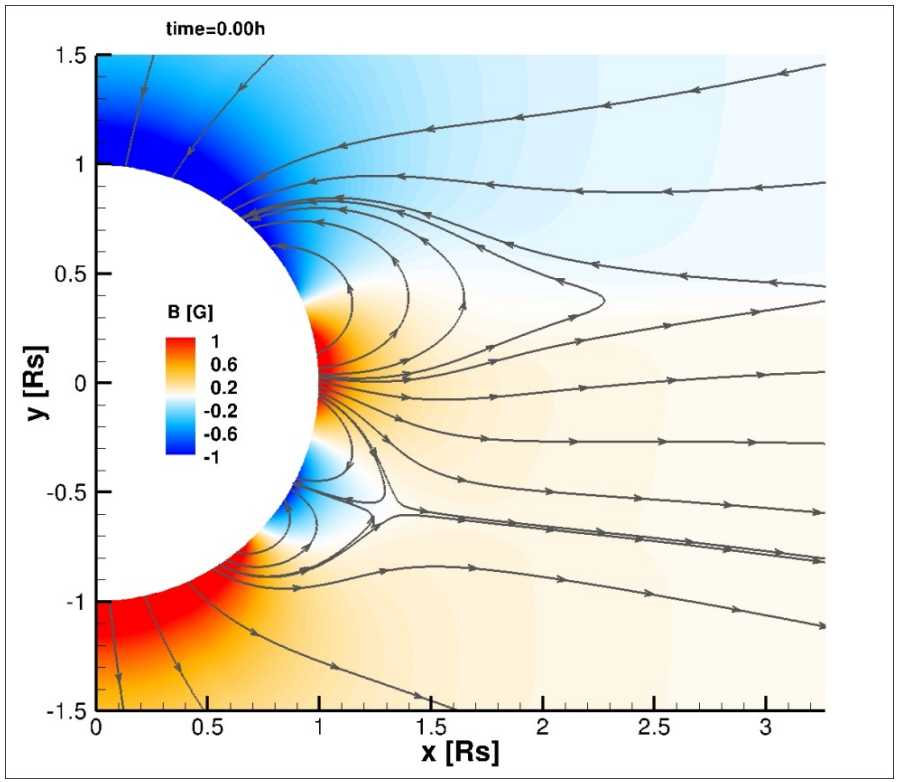

- PFSS extrapolation l=10, m=10.
- A helmet streamer that is shifted northward.
- A pseudostreamer overlying the AR.
- Loop system connecting the negative polarity of the AR to the global magnetic field

- Initial condition for the simulation
- Key properties, i.e., the northward shift of the helmet streamer and the pseudostreamer, are all reproduced.
- But not the azimuthal component of the field.

Dynamical evolution (I)

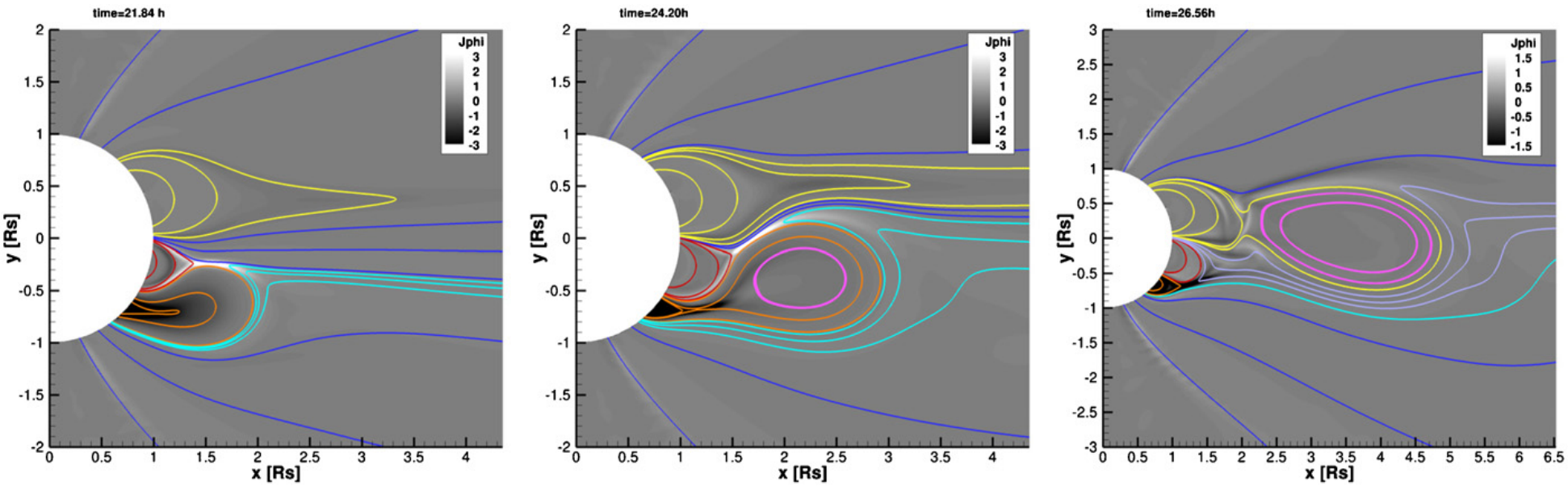

- We impose localized shearing motions along the polarity inversion line of the AR.
- The X-point is shifted northwards and interchange reconnection sets in.
- The southern arcade starts to rise and the prominence is formed.
- Southern arcade flux is transferred partially to the central arcade and partially to the open field.
- The reconnection at the X-point results in a pressure imbalance → northward shift of the CME.
- The newly formed open flux of the southern coronal hole reconnects with the flux of the central arcade definitely separating the fluxrope from its formation location and the fluxrope gets absorbed in the northern helmet streamer.

Dynamical evolution (II)

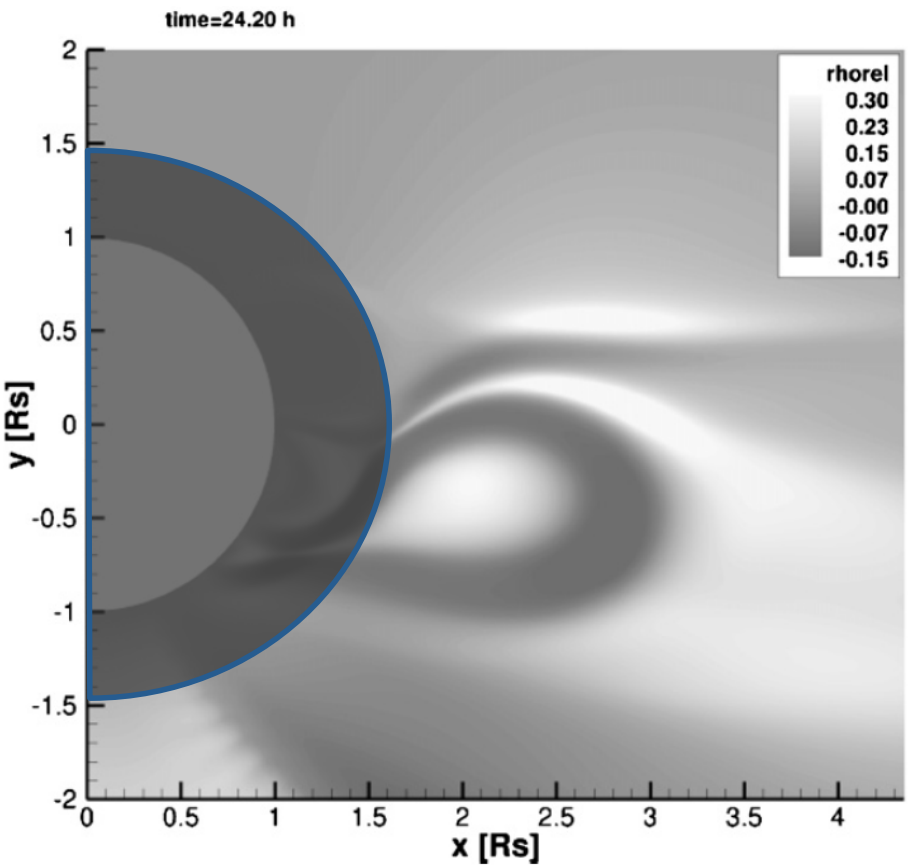

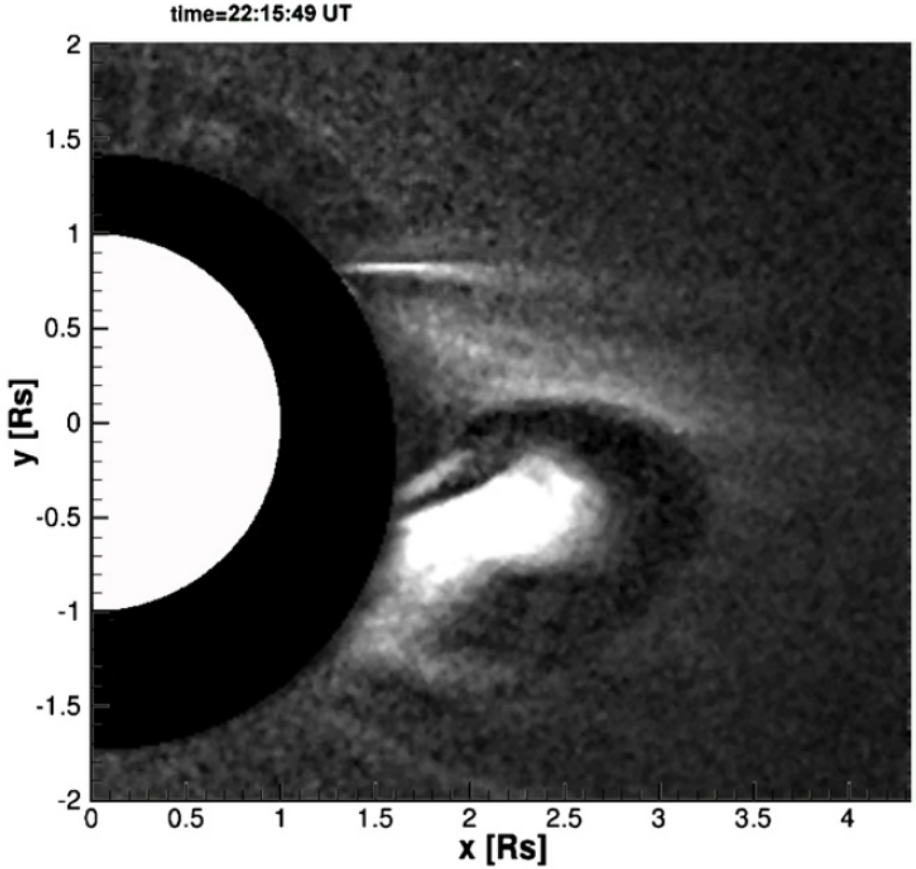

- When the flux rope is propagating within the COR1 FOV, the high-density core as well as the three-part structure are clearly visible.
- An increase in the relative density in the X-point is visible both in the observations and simulations.

Radial & Latitudinal Evolution

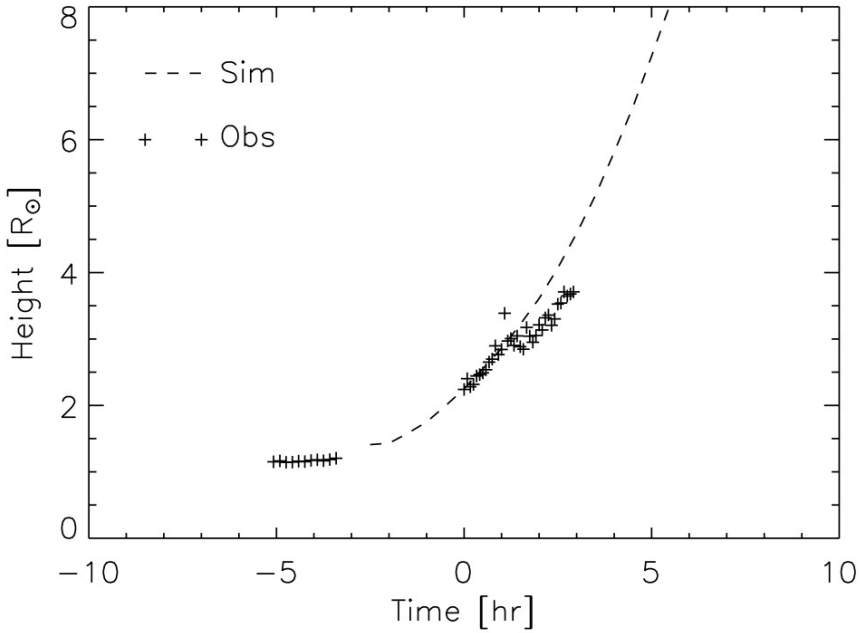

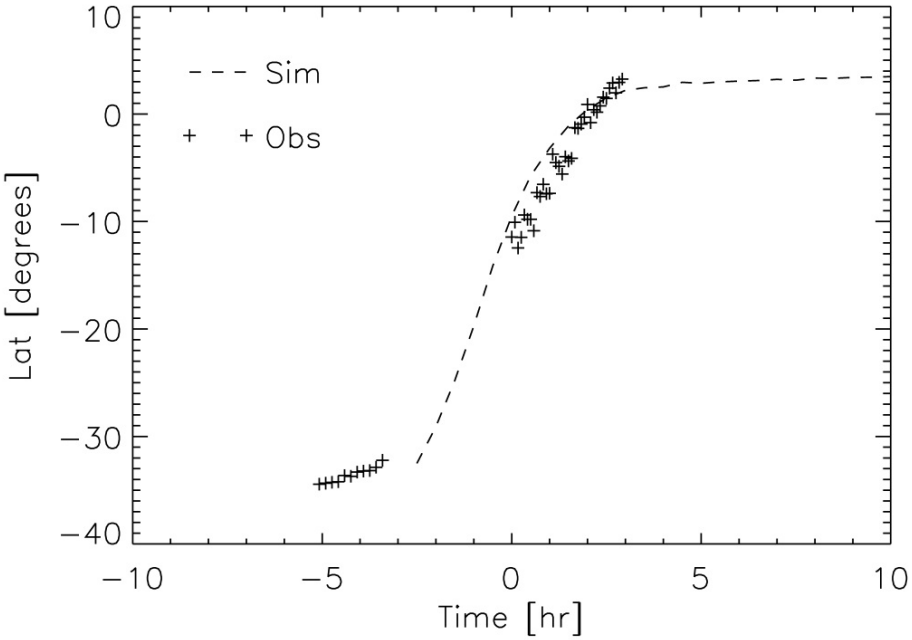

- Time zero is 20:00 UT on 2009 September 21, i.e. the time at which the CME was at $2.25R_0$.
- It takes about 6 hr to reach an altitude of $4R_0$ and both CMEs are slow.
- The simulation well reproduce the evolution of the CME in the COR1 FOV
- The CME is deflected of ~20° within the first $2.25R_0$ and of ~16° within the COR1 FOV.

The role of the global field (I)

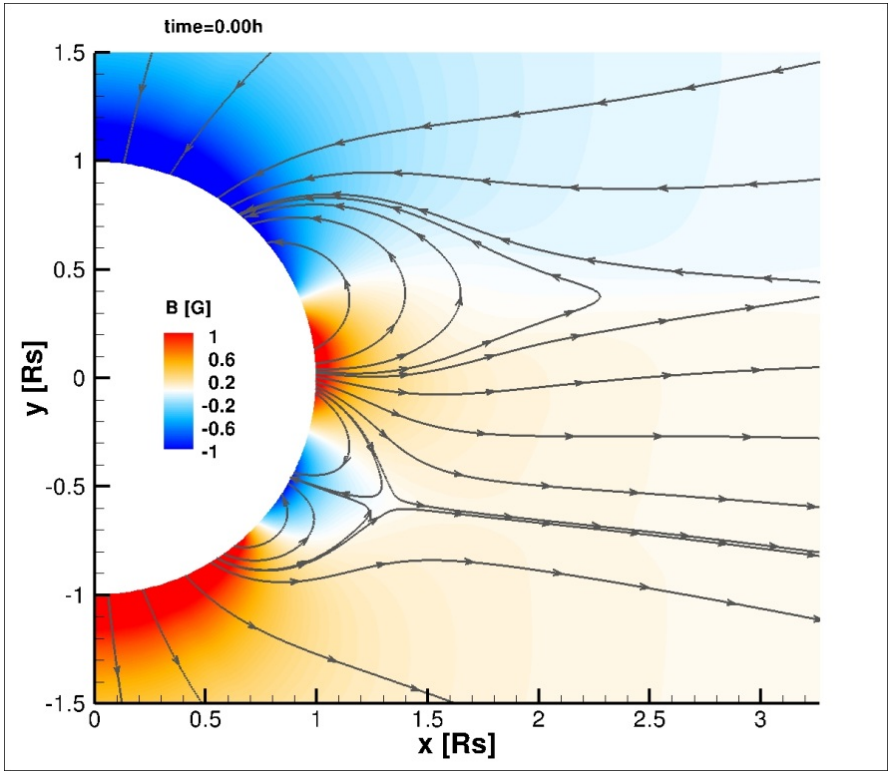

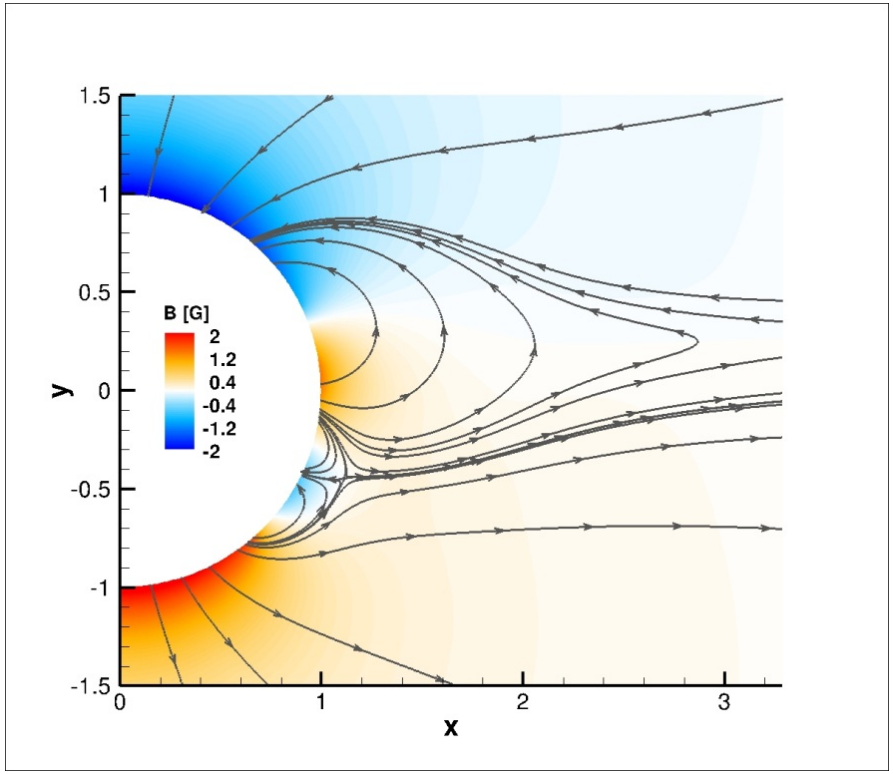

- We increase the global field of about 33 %.
- The null-point is located within the closed general dipole flux and a breakout topology configuration is obtained.
- No pseudo-streamer present.

The role of the global field (II)

- Due to the increased magnetic tension of the overlying field, the CME1 undergoes a more sudden deflection towards the equator .

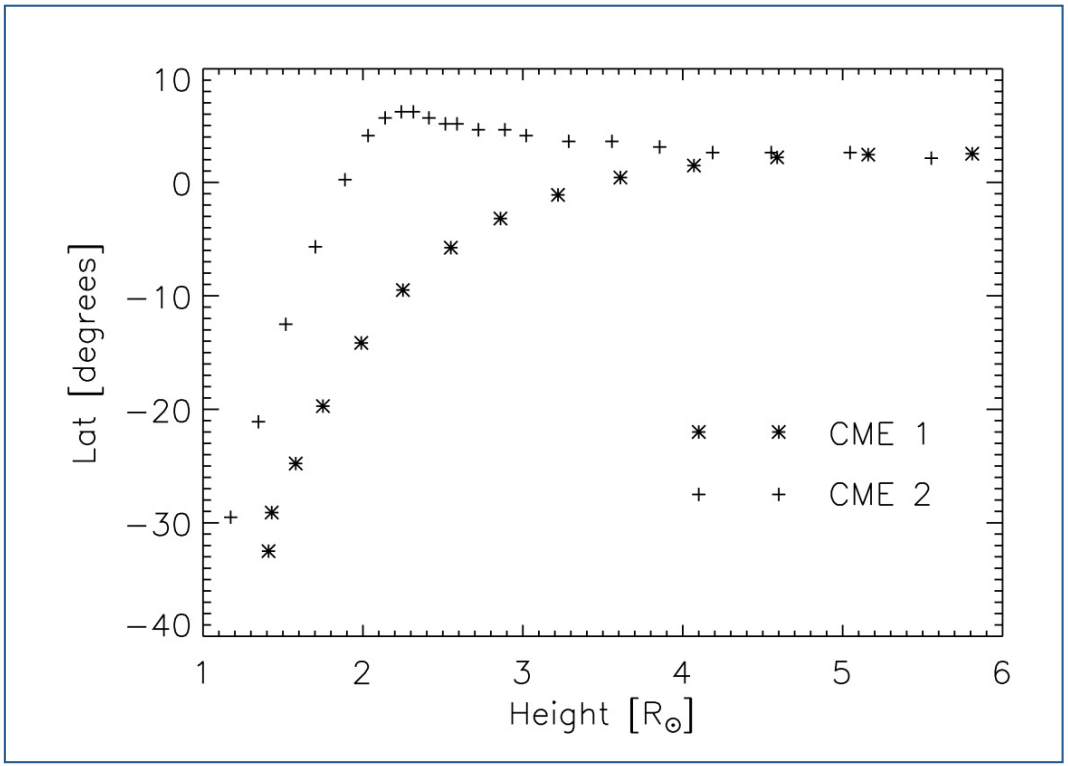

Conclusions

- During solar minimum conditions the global field plays a crucial role in the evolution of CMEs.
- How rapidly CMEs undergo the latitudinal migration depends on the strength of both the large-scale coronal magnetic field and the magnetic flux of the erupting filament.
- Asymmetric convergence motions involving only part of the AR flux can initiate CMEs.
- At the moment the flare reconnection sets in, we find that the unsigned flux around the polarity inversion line decreases by about 4%: a small amount of flux cancellation is sufficient to trigger a large disruption.
- Post-flare loops, the transition from initially high sheared configuration to a more potential one proceeds in a gradual fashion, starting from the loops closer to the inner boundary to loops that extend higher up in the solar atmosphere.
- The inclusion of a finite-β plasma allows a better understanding of the reconnection-related magnetic energy decrease.

Zuccarello, F. P. et al. 2012, ApJ, 744, 66
Zuccarello, F. P. et al. 2012b, ApJ, 758, 117

Thank you !

Francesco P. Zuccarello

Centre for mathematical Plasma Astrophysics, KU Leuven

francesco.zuccarello@wis.kuleuven.be